The influence of a cubic building on a roof mounted wind turbine

Micallef, Daniel; Sant, Tonio; Ferreira, Carlos

Citation (APA)
Micallef, D., Sant, T., & Ferreira, C. (2016). The influence of a cubic building on a roof mounted wind turbine. *Journal of Physics: Conference Series*, *753*(2), Article 022044. https://doi.org/10.1088/1742-6596/753/2/022044

Important note
To cite this publication, please use the final published version (if applicable).
Please check the document version above.

The influence of a cubic building on a roof mounted wind turbine

Daniel Micallef, Tonio Sant, Carlos Ferreira

(1) Department of Environmental Design, Faculty for the built environment, University of Malta.
(2) Department of Mechanical Engineering, Faculty of engineering, University of Malta.
(3) Department of Aerodynamics, Wind Energy and Propulsion, Delft University of Technology.

E-mail: `daniel.micallef@um.edu.mt`

Abstract.
    The performance of a wind turbine located above a cubic building is not well understood. This issue is of fundamental importance for the design of small scale wind turbines. One variable which is of particular importance in this respect is the turbine height above roof level. In this work, the power performance of a small wind turbine is assessed as a function of the height above the roof of a generic cubic building. A 3D Computational Fluid Dynamics model of a 10m x 10m x 10m building is used with the turbine modelled as an actuator disc. Results have shown an improvement in the average power coefficient even in cases where the rotor is partially located within the roof separation zone. This goes against current notions of small wind turbine power production. This study can be of particular importance to guide the turbine installation height on building roof tops.

1. Introduction and objectives
The aerodynamics of small and micro-scale wind turbines located on top of a cubic building block has had little attention in the literature. It is hypothesised that there is a specific critical height of the turbine from the roof above which the turbine performance starts to be enhanced. The interaction between the separation bubble over the roof of a building and a wind turbine can be either positive when flow is augmented or negative when the performance of the turbine is undermined by its interaction with the zone of separated flow.
    The objectives of this work can be summarised as follows: (1) To determine the influence of the wind turbine-to-roof interaction on the turbine power coefficient and (2) To establish a relationship between turbine height from a building roof and the power performance.

2. State of the art
Roof-top mounted wind turbines offer significant potential in reducing the carbon footprint of buildings, yet their cost-effectiveness is impacted by having to operate in the lower regions of the atmospheric boundary layer where wind flows are lower and more turbulent. Computational Fluid Dynamics (CFD) is an indispensable tool for identifying optimal locations for mounting wind turbines, taking advantage of flow augmentations induced by buildings. Some of the earliest analysis involving the application of CFD as a tool for siting of building-mounted wind

turbines were presented by [1]. These have been followed by comprehensive works some of which have been reviewed by [2] and [3]. [4] applied a CFD RANS solver with an SST $k - \omega$ turbulence model to simulate the wind flows over a cluster of houses in a suburban environment to investigate the influence of the rooftop geometry on the wind flow conditions. It was found that houses with flat roofs tend to result in higher power for the same turbine hub elevation than those having pitched or pyramidal roofs. The numerical predictions have also indicated that flat roofs generally cause lower turbulence intensities downstream, resulting in a more consistent power output. [5] conducted further analysis to cover more roof geometries, including vaulted, domed and wedged shaped. [6] extended the use of CFD by for micro-siting of small roof-top wind turbines over a relatively large build-up area by coupling ANSYS®CFX to the wind atlas software WAsP®. Although the above works assessed in detail flow conditions around the buildings, the localised effects resulting from the presence of the wind turbine have so far not given too much attention. Existing literature suggests the need for further work using CFD to examine turbine wake aerodynamics in the presence of buildings.

3. Method

3.1. Wind turbine model

An Actuator Disc (AD) model as described in various sources in literature such as [7, 8, 9] is used to model the turbine loading on the air. The turbine is assumed to have a radius of 1m. As described in Troldborg et al. [8], the axial thrust and power coefficient are defined respectively:

$$C_T(r, \theta) = \frac{f(r, \theta)}{\frac{1}{2}\rho V_0^2(r, \theta)} \tag{1}$$

$$C_P(r, \theta) = \frac{f(r, \theta)V_z(r, \theta)}{\frac{1}{2}\rho V_0^3(r, \theta)} \tag{2}$$

where f is the thrust per unit area $\frac{dT}{dA}$, ρ is the air density, r is the radial location from the rotor's centre, V_z is the axial velocity at the rotor disc, and V_0 is the reference free stream velocity. The choice of the upstream position of where to define the wind velocity V_0 might not be as trivial as when the turbine is investigated in isolation. When the building is present, the definition of the 'free' stream becomes somewhat ambiguous in that the free stream is usually defined as the velocity at the rotor hub position without the turbine influence. The sensitivity to the choice of this upstream position will be discussed in another section.

The thrust coefficient is assumed to be fixed and uniform across the entire rotor disc, with the value corresponding to that for optimal operation, $C_T(r, \theta) = 0.89$. This way the prescribed loading (per unit area) $f(r, \theta)$ could be calculated from eqn. 1. In reality, this condition is necessary in order to be able to establish the thrust and hence be able to apply the appropriate load on the actuator disc. This is also the approach followed by [8] for the application to the effects of sheared free-stream velocities.

A Gaussian blur along the axial direction is used to remove the disc pressure jump singularity. Due to the various descriptions of this approach in previous literature, the readers are referred to sources such as Mikkelsen [7], Troldborg et al. [8] and Micallef et al. [10]. The Computational Fluid Dynamics (CFD) model is implemented using the commercial software ANSYS®Fluent 15.0. While in the work of Troldborg et al. [8], the definition of the free stream velocity $V_0(r, \theta)$ was simply taken as the velocity corresponding to the wind speed profile far upstream from the turbine, in this case, such a definition becomes less clear. This is due to the presence of the building bluff body. The sensitivity of the result to this issue will be explored further in this paper.

3.2. Assumptions and parameters used

To maintain focus on the research objective, a number of parameters are assumed to be fixed. These include, the position of the turbine along the roof (assumed to be located at the center of the roof), the dimensions of the cubic building ($10m \times 10m \times 10m$) and the wind speed profile (6m/s wind speed at the reference hub height of 14m). An isolated building case is also considered and hence there is no upstream turbulence generation due to the presence of other buildings or structures. This corresponds to $Re_{turbine} = 844,648$ based on the turbine diameter and $Re_{building} = 4,223,270$ on the basis of building characteristic dimension of 10m. At such high Re numbers, the thrust experienced by the rotor disc and the pressures acting on the building are well known to be Re number independent and hence the use of a single wind speed is well justified.

3.3. Problem discretisation and verification of solution

Two types of meshes were used with and without the building being present. A structured mesh approach was used to minimise the number of cells and improving convergence trends. Fig. 1 shows two views of the mesh employed near and around the building envelope. Some high aspect ratio cells resulted which could have created some numerical convergence issues for regions where the flow is not aligned with the long edge of the cell. In this case however, the simulation converged without any noticeable problems. A point worth noting is that when the use of the RNG $k - \epsilon$ turbulence model was used, the simulation showed some numerical instability.

The turbine actuator disc location is also indicated. To ensure mesh independence the guidelines by Roache & Patrick [11] and Celik et al.[12] were used and the final mesh is depicted in fig. 1 which includes the detail of the turbine region.

The domain size used follows the guidelines of Franke et al.[13] and is equivalent to $6H$ upstream from the building position, $12H$ downstream from the building to the outlet, $6H$ from the sides of the building to the side of the domain, $6H$ from the building roof to the domain top surface. For all simulations, both convergence residuals were monitored as well as velocities at different locations in the flow field. The residuals were all below 10^{-4} and showed convergence after around 5000 iterations. The velocities at the monitor points also converged satisfactorily without showing any further variations with increased iterations beyond around 5000, depending on the simulation case.

3.4. Turbulence and wall modelling

The correct modelling of turbulence is important in this context for two main reasons. First, the correct prediction of the separation zone on the roof of the building is well known to be strongly dependent on the turbulence closure model used (see Yu et al. [14] and Richards [15]). The Reynold's Averaged Navier Stokes (RANS) equations are used with the Realizable $k - \epsilon$ model. The main reason for using this model is that $k - \epsilon$ models are known to be computationally efficient since standard wall functions can be used, requiring less refinement close to walls. The RNG $k - \epsilon$ model ([16]) was also considered since this is known to reproduce the separation zone more accurately over the roof [17]. This attempt failed due to numerical instabilities after some iterations.

In general, all $k - \epsilon$ models including the realizable $k - \epsilon$ used here are known (see Shao et al.[18]) to over-estimate the turbulent kinetic energy in the separated region. Nonetheless, for this study, the accurate prediction of the flow within this separation zone is not really important since it is not of engineering interest to place the turbine within this zone. The separation zone height is more important in this case but the literature is limited in this regard. Another fact to consider is that the separation bubble above the roof can be periodic and while the RANS equations provide mean flows, in reality the turbulent region above roof level shows fluctuations
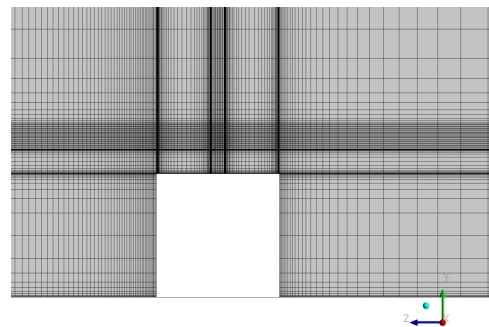
(a) side elevation
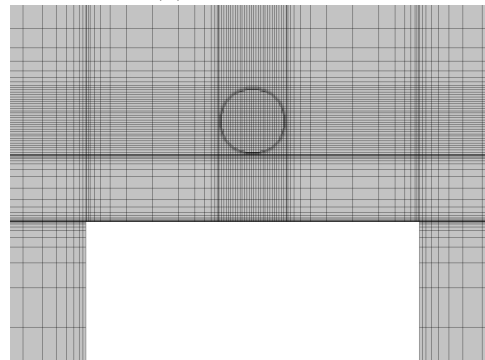
(b) front elevation showing actuator disc positon

Figure 1: Meshed model for turbine height to building height ratio $H_T/H = 1.4$.

which can only be captured by means of for instance Large Eddy Simulation (LES). Another reason for the importance of the correct modelling of turbulence is due to the wake dissipation from the turbine and how this interacts with the separated flow resulting from the building. This might have important effects on the turbine performance itself.

The inflow condition to the domain has a prescribed shear. While the influence of shear is barely noticeable for a small turbine(difference in wind velocity between the disc edges is less than 0.1m/s), the flow separation on the building roof will be affected by this profile. No inlet atmospheric boundary layer turbulence is assumed as otherwise the choice of turbulence model becomes invalid due to the well known inability for the $k - \epsilon$ model to predict the rotor wake under the influence of the much larger atmospheric turbulent length scales (see for example Kasmi & Masson [19] and Cabezon et al. [20].

Walls are modelled using standard wall functions. The mesh was refined close to walls such that the dimensionless wall distance y^+ was maintained in the range $30 < y^+ < 300$ at the walls.

3.5. Wind profile model
A logarithmic wind profile is used following the best practice guidelines of Franke et al. [13]:

$$V_0(z) = \frac{u_*}{\kappa} log \left(\frac{y + y_0}{y_0} \right) \tag{3}$$

Where u_* is the friction velocity, κ is the von karman constant (0.4187), y is the vertical distance from ground level, y_0 is the aerodynamic roughness length. The reference wind velocity at a (reference) height of 14m above ground level is 6m/s.

Both the turbulent wind kinetic energy k as well as the wind turbulent dissipation rate ϵ had to be kept zero in order to maintain the validity of using a Realizable $k - \epsilon$ to model the wake from the turbine correctly without causing quick dissipation due to the much larger turbulent scales of the wind.

In order to ensure lack of horizontal wind homogeneity the guidelines by [21] are used by modifying the ground roughness height. This is possible provided that standard wall functions were used. An empty domain simulation was carried out to ensure that the wind profile is maintained homogeneous from inlet to the building location.

3.6. Simulation cases
The case of an isolated turbine at the reference height of 14m is first simulated for comparison purposes. This is performed with a wind speed profile corresponding to eqn. 3. Another five cases were tested with turbine height to building height ratios of $\frac{H_T}{H} = 1.2, 1.3, 1.4, 1.5, 1.7$.

4. Results
4.1. Flow characteristics
A comparison of the flow field between the different positions of the turbine is shown in fig.2. The first figure shows the case of an isolated turbine under the same wind profile as used for the simulations with the building included. At $H_T = 1.2H$, the turbine is practically entirely within the roof separation zone. The interaction between the wake from the turbine and the flow field results from the roof separation zone is very complex but the resulting velocities experienced by the turbine are very low, resulting in a low power extraction or even possibly in propeller mode operation. For $H_T = 1.3H$ the rotor is only partially within the roof separation zone and still the interaction between the turbine streamtube and the separated flow from the roof is clearly visible. When the turbine height is increased to $H_T = 1.4H$ which corresponds to the reference height, the turbine streamtube and the separation zone from the roof are clearly distinct but are influenced by each other. This causes the turbine wake to be pushed upwards while the turbine experiences a higher inflow at the upstream location. As the turbine height is increased further, the interaction between the wake and the separated zone becomes less apparent but the turbine experiences a slightly higher free stream velocity due to the atmospheric boundary layer profile.

Fig. 3 shows a comparison of the velocities along the wind direction between the case where there is no turbine and the velocity profile when it is included at different heights above roof level. These velocity profiles are important to establish the influence of the turbine on the roof separation mechanism. The velocity profiles are plotted at the center of the roof at the turbine location. The plots show the vertical distance above roof level normalized with the building height $\frac{Y}{H}$ against the normalized velocity $\frac{V_z}{V_0}$. The turbine actuator disc location is indicated in each case with red dotted lines.

The height of the separation zone from the roof is 3m above roof level. When the turbine is centred at $\frac{Y}{H} = 1.2$, there is a substantial interference on the velocity profile just above the roof and above the turbine. Also, the difference in velocity between the undisturbed separation zone and the case with the turbine included at such a close distance to the roof is around $\frac{V_z}{V_0} = 0.5$. When the turbine height is $\frac{Y}{H} = 1.3$, the velocity along the rotor disc is rather uniform but reduces dramatically in the region where it interacts with the roof separation zone. It is also clear that the influence of the separation zone is at a slightly lower height than undisturbed separation zone from the building.

At a turbine height of $\frac{Y}{H} = 1.4$ and above, the turbine does not influence the separation zone height appreciably and the velocity profiles below the turbine position agree with those of the undisturbed building case.
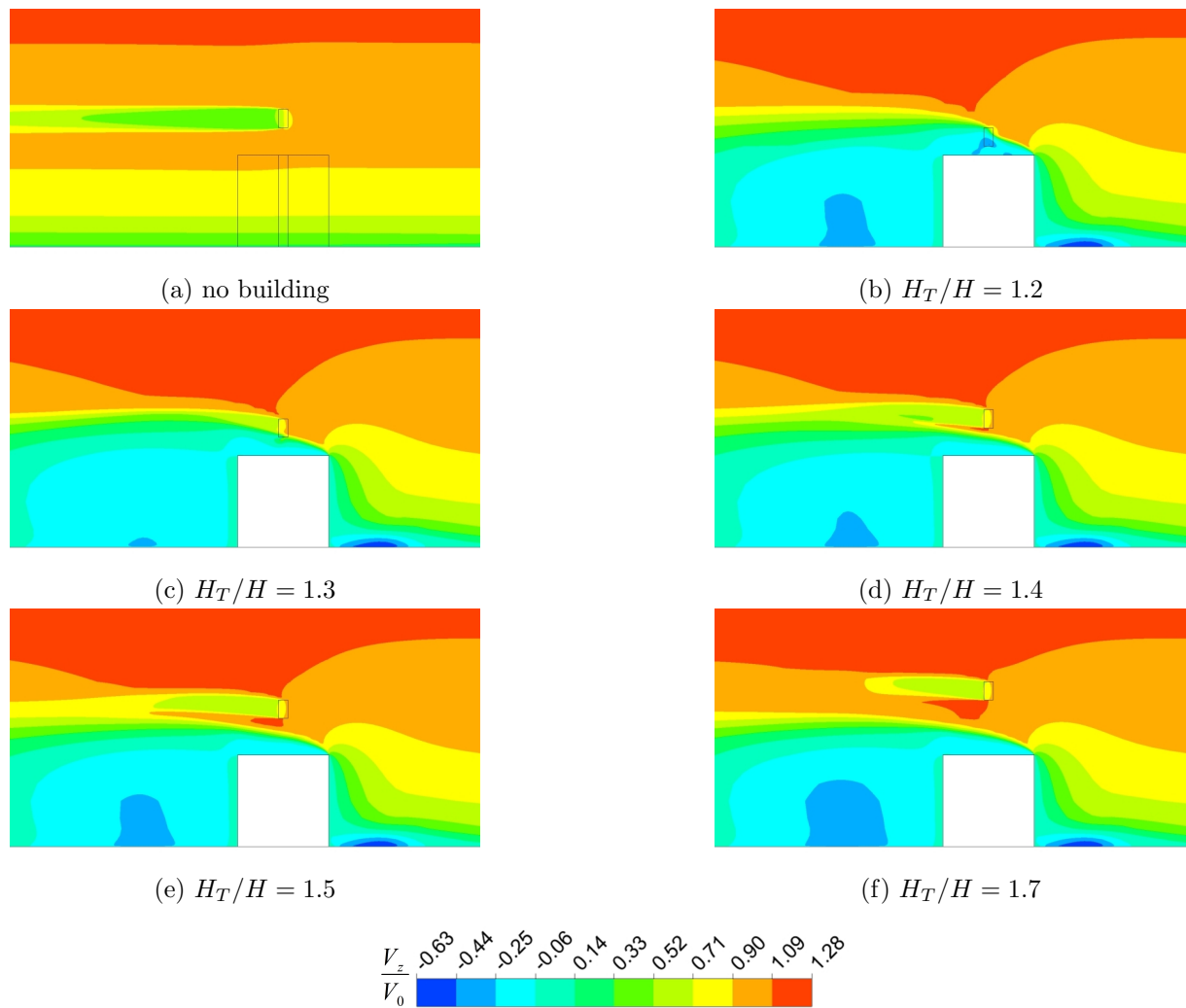
(a) no building

(b) $H_T/H = 1.2$

(c) $H_T/H = 1.3$

(d) $H_T/H = 1.4$

(e) $H_T/H = 1.5$

(f) $H_T/H = 1.7$

$\frac{V_z}{V_0}$ -0.63 -0.44 -0.25 -0.06 0.14 0.33 0.52 0.71 0.90 1.09 1.28

Figure 2: Velocity V_z (in the wind direction) normalized with the reference free stream velocity of 6m/s. The wind direction is from right to left. Results are shown for the isolated turbine at a reference height of 1.4 times the building height and also for the turbine-building configurations with the turbine being at different heights from the roof.

4.2. Power, thrust and sensitivity analysis

In order to assess the performance of the turbine with increasing height from the roof level, the power extracted from each turbine element is defined as:

$$dP(r,\theta) = C_P(r,\theta)\frac{1}{2}\rho V_0^3(r,\theta)dA \qquad (4)$$

where dA is the element area. The average power is thus

$$\overline{P} = \frac{1}{A}\int\int C_P(r,\theta)\frac{1}{2}\rho V_0^3(r,\theta)dA \qquad (5)$$

A variable R_P is defined to compare between the average power of the turbine-building configuration and the average power from an isolated turbine $\overline{P}_{free}$. This is therefore defined as follows:
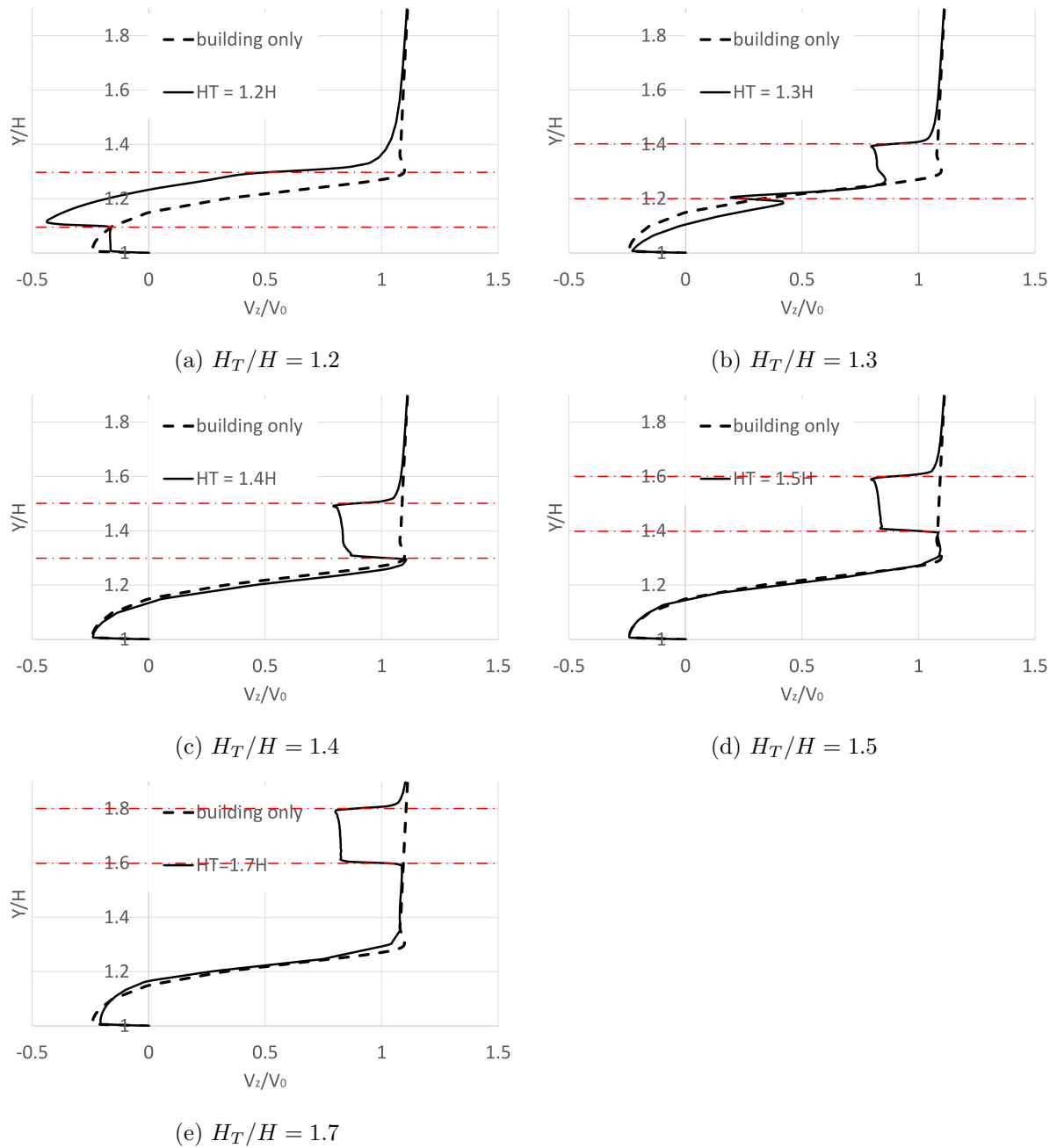
Figure 3: Plot of the y position normalized with the building height H against velocity V_z normalized with the reference free stream velocity(6m/s). The profiles are shown at the rotor position. Each result is compared with the case of no turbine. The turbine location is indicated by the dotted red lines. The location of the turbine along the free stream direction is at the centre of the building.

$$R_P = \frac{\overline{P}}{\overline{P}_{free}} \qquad (6)$$

Similarly for the thrust we can write:

$$\overline{T} = \frac{1}{A} \int \int C_T(r,\theta)\frac{1}{2}\rho V_0^2(r,\theta)dA \qquad (7)$$

The ratio of the averaged turbine thrust ($\overline{T}$) when the building is present and that when the turbine is not exposed to the building influence ($\overline{T}_{free}$) is given by

$$R_T = \frac{\overline{T}}{\overline{T}_{free}} \qquad (8)$$

The results for R_P and R_T with turbine height are given in fig. 4 and fig. 5 respectively. Two cases are shown, the first where the reference upstream position of the wind profile V_0 is chosen at $6m$ and the second when it is chosen close to the inlet of the domain at $20m$, far from the influence of both the building and turbine. At $6m$ upstream, the wind velocity V_0 is uninfluenced by the turbine but influenced by the building. From the results it is clear that the influence of the choice of upstream position starts only to be appreciable at $\frac{H_T}{H} = 1.3$ or below, when the separation zone from the roof starts influencing the wind speed profile. At turbine heights higher than this, the definition of the velocity V_0 is uninfluenced by the separation zone and hence the choice of upstream position becomes less important for the actuator disc model employed here.

There is a positive effect on power as the turbine height is $\frac{H_T}{H} > 1.3$ this is despite the fact that (as mentioned earlier) the separation zone from the roof without a turbine has a height of 3m which would correspond to the disc centre. When an upstream position of 20m is chosen, a slight improvement over the free turbine performance is also observed. As the height of the turbine is increased, the performance becomes superior due to the effect of the increased wind velocity with height. The effect of the building beyond the separation zone is also to provide some flow augmentation and therefore the reason for the increased performance is twofold.

As regards the rotor thrust, since the actuator disc model was implemented with a fixed C_T of 0.89, the thrust will be simply a quadratic function of the wind velocity. Since the definition of the free turbine is at $\frac{H_T}{H} = 1.4$, for all turbine heights below this, the thrust will be lower than the free turbine case. For the $\frac{H_T}{H} = 1.5$ case, $R_T \approx 1$ and increases beyond 1 as the height is increased.T his is an indication of how much you need to increase the heigh with the building to have the same thrust of the isolated turbine. In this case, the choice of the reference upstream position becomes even more important due to this quadratic relationship between the thrust and the wind velocity V_0.

5. Discussion
It is interesting to note, particularly from the results presented earlier (see figure 2), that the turbine and building flows are highly coupled. The separation zone behind the building can be seen to be influenced by this. When the turbine-to-building height is 1.2, it was observed that the rotor acts as a propeller and a larger wake region is observed. When $H_T/H = 1.3$ the wake region from the building is somewhat more suppressed and higher velocities can be observed. As the turbine height increases above the building roof, more negative velocities can be observed in the building wake. This is due to the lower blockage (localised in that region) caused by the building and turbine configuration.

A sensitivity analysis on the wind profile chosen is reserved for future work since this might have important implications on the separation zone on the roof which could lead to different
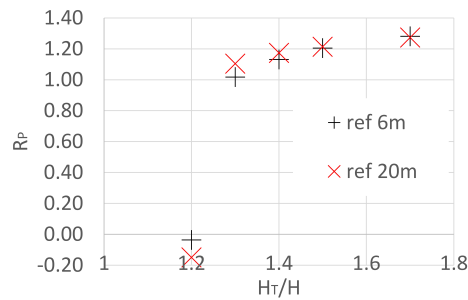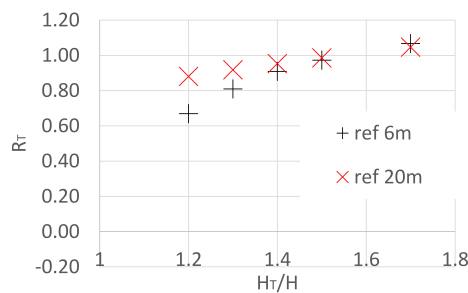
Figure 4: Variation of R_P with turbine height.

Figure 5: Variation of R_T with turbine height.

conclusions regarding the turbine height which can be considered acceptable for improved performance. In addition this may have an impact on power.

While the actuator disc approach can be rather simplistic for such complex scenarios found in urban environments, a full rotor CFD approach could be an interesting point of investigation in order to validate and compare results. In addition the use of Blade Element Momentum Methods (BEM) with the inflows found in this work could be also useful in order to compare how different approaches can be utilized. This is however reserved as additional future work.

6. Conclusion

Small wind turbines for urban wind energy exploitation have been developed by industry in order to address the energy challenges of cities and urbanised zones. The efficiency of such turbines is in many cases hampered due to the wind condition present at the turbine site. The aerodynamic design of such turbines usually attempts to address this issue but aerodynamic knowledge of the wind turbine to building interaction is lacking. From this paper the following conclusions may be drawn:

- While it is well known that increasing turbine height above roof level will exploit the higher wind speeds found at higher altitudes to the atmospheric boundary layer, this paper provides an indication of the lower height limit below which turbine performance deteriorates dramatically.

- This height does not simply correspond to the height of the separation zone above roof level for a building without a turbine. In the case presented, while the separation zone height for an isolated building is 3m above roof level, the turbine was still predicted by the CFD AD model to perform similarly.

- As turbine height increases above roof level, there is a combined effect of increased wind velocity due to the atmospheric boundary layer as well as due to the building presence.

There are a number of issues which this approach fails to take into account including for instance: (i) the effect of atmospheric turbulence, (ii) the influence of other structures/buildings (iii) the influence of varying wind directions.

While all of the above can have significant repercussions on the results presented in this work, the approach used here is based on a methodical consideration of the influence of the building on turbine performance. The effect of atmospheric turbulence can be treated by the use of more advanced turbulence models such as Large Eddy Simulation (LES).

The paper explores a 'back to basics' and integrated approach in urban wind energy where urban and turbine aerodynamics are not treated separately as with most of the studies found in literature.

References

[1] Mertens S 2003 *Wind Engineering* **27** 507–518 ISSN 0309-524X URL http://multi-science.metapress.com/openurl.asp?genre=article&id=doi:10.1260/030952403773617472
[2] Walker S L 2011 *Energy and Buildings* **43** 1852–1862 ISSN 03787788 URL http://www.sciencedirect.com/science/article/pii/S0378778811001101
[3] Ayhan D and Salam A 2012 *Renewable and Sustainable Energy Reviews* **16** 1040–1049 ISSN 13640321
[4] Ledo L, Kosasih P B and Cooper P 2011 *Renewable Energy* **36** 1379–1391 ISSN 09601481 URL http://dx.doi.org/10.1016/j.renene.2010.10.030
[5] Abohela I, Hamza N and Dudek S 2013 *Renewable Energy* **50** 1106–1118 ISSN 09601481 URL http://dx.doi.org/10.1016/j.renene.2012.08.068
[6] Tabrizi A B, Whale J, Lyons T and Urmee T 2014 *Renewable Energy* **67** 242–251 ISSN 09601481 URL http://dx.doi.org/10.1016/j.renene.2013.11.033
[7] Mikkelsen R 2003 *Actuator Disc Methods Applied to Wind Turbines* Ph.D. thesis Technical University of Denmark
[8] Troldborg N, Gaunaa M and Mikkelsen R 2010 *Torque 2010, The science of making torque from wind, EWEA* p271–297
[9] Lignarolo L E, Mehta D, Stevens R J, Yilmaz A E, van Kuik G, Andersen S J, Meneveau C, Ferreira C J, Ragni D, Meyers J, van Bussel G J and Holierhoek J 2016 *Renewable Energy* **94** 510–523 ISSN 09601481 URL http://www.sciencedirect.com/science/article/pii/S0960148116302543
[10] Micallef D and Sant T 2015 *Renewable Energy* **83** 737–748 ISSN 09601481 URL http://linkinghub.elsevier.com/retrieve/pii/S0960148115003936
[11] Roache P J 1998 *Verification and Validation in Computational Science and Engineering* (Hermosa Publishers) pp 107–141
[12] Celik I B, Ghia U, Roache P J, Freitas C J, Coleman H and Raad P E 2008 *Journal of Fluids Engineering* **130** 1
[13] Jörg Franke, Antti Hellsten, Heinke Schlünzen B C 2007 *Best Practice Guideline for the Cfd Simulation of Flows in the Urban Environment Quality Assurance and Improvement of* May ISBN 3000183124
[14] Yu Y, Barron R M and Balachandar R 2012 Numerical Prediction of Pressure Distribution on a Cube Obstacle in Atmospheric Boundary Layer Flow *Proceedings from the CFD Society of Canada conference*
[15] PJ Richards A Q and Parker S 2002 *Wind and Structures, An International Journal* **5** 177–192
[16] Yakhot V, Orszag S A, Thangam S, Gatski T B and Speziale C G 1992 *Physics of Fluids A: Fluid Dynamics (1989-1993)* **4**
[17] Blocken B 2014 *Journal of Wind Engineering and Industrial Aerodynamics* **129** 69–102 ISSN 01676105
[18] Shao J, Liu J and Zhao J 2012 *Building and Environment* **57** 145–155 ISSN 03601323 URL http://www.sciencedirect.com/science/article/pii/S0360132312001370
[19] El Kasmi A and Masson C 2008 *Journal of Wind Engineering and Industrial Aerodynamics* **96** 103–122 ISSN 01676105 URL http://www.sciencedirect.com/science/article/pii/S0167610507000943
[20] D Cabezon, J Sanz, I Marti and Crespo A 2009 Cfd modeling of the interaction between the surface boundary layer and rotor wake. comparison of results obtained with different turbulence models and mesh strategies *EWEC, Marseille*
[21] Blocken B, Stathopoulos T and Carmeliet J 2007 *Atmospheric Environment* **41** 238–252 ISSN 13522310 URL http://www.sciencedirect.com/science/article/pii/S135223100600834X